CTU Journal of Innovation and Sustainable Development
ISSN 2588-1418 | e-ISSN 2815-6412

DOI:10.22144/ctujoisd.2025.012

Using efficient bimetallic FeCo-ZIFs catalyst for Ciprofloxacin degradation in the presence of potassium peroxydisulfate

Cao Dang Hoang An[1,2], Le Thi Anh Thu[1,2], Pham Thi Truong An[1,2], Ha My Tien[1,2], Nguyen Thi Kim Ngan[1], Cao Luu Ngoc Hanh[1], and Dang Huynh Giao[1,2*]

[1]*College of Engineering, Can Tho University, Viet Nam*

[2]*Applied Chemical Engineering Lab, College of Engineering, Can Tho University, Viet Nam*

**Corresponding author (dhgiao@ctu.edu.vn)*

Article info.

Received 15 Aug 2024
Revised 5 Sep 2024
Accepted 17 Feb 2025

Keywords

Bimetallic FeCo-ZIFs, catalyst, ciprofloxacin, potassium peroxydisulfate, zeolite imidazole frameworks

ABSTRACT

Solvothermal synthesis was used for the successful manufacture FeCo-ZIFs bimetallic materials. The materials' properties were determined using a variety of techniques, including Fourier-transform infrared spectroscopy (FT-IR), energy dispersive X-ray spectroscopy (EDX), powder X-ray diffraction (PXRD), scanning electron microscopy (SEM), thermogravimetric analysis (TGA), and nitrogen adsorption ability. The obtained FeCo-ZIFs were acted as catalysts to remove Ciprofloxacin in aqueous media with high efficiency. It showed that the decomposition efficiency of Ciprofloxacin reached 92.1% with a weight of 0.4 g/L FeCo-ZIFs, and 0.3 g/L potassium peroxydisulfate for 30 min at room temperature (30±2°C). According to research, this is the first time FeCo-ZIFs was applied to treat Ciprofloxacin.

1. INTRODUCTION

The fluoroquinolone antibiotic ciprofloxacin (CIP) is one of the antibiotics that has been found to be present in environmental residues. CIP's antibacterial action toward both gram-negative and gram-positive bacteria stems from being able to inhibit enzymes involved in bacterial nucleic acid synthesis. This antibiotic has been found in microgram concentrations in drinking water as well as wastewater from drinking establishments, hospitals, and wastewater treatment plants (Farghal et al., 2021). Up to now, there have been numerous ways to treat these dangerous remaining chemicals, such as coagulation, membrane separation, advanced oxidation, etc. (Mondal, Saha, & Sinha, 2018). These techniques do have certain drawbacks, though. More specifically, the activated carbon adsorption technique or membrane filtration is highly costly and not feasible for business. while the oxidation method can produce hazardous and difficult-to-decompose products. On the other hand, the remaining methods require complex experimental conditions and equipment (Méndez-Paz et al., 2005). Consequently, this has become essential to explore methods to treat these dangerous substances while also getting around the drawbacks of the previous approaches. The creation of novel material groups has created numerous research avenues that are seen to be promising and effective solutions to the challenge of treating environmental pollution, given the current complicated developments in environmental pollution, particularly water contamination. Among new materials, metal-centered organic frameworks (MOFs), in general and zeolite-structured ZIFs, in particular, have several outstanding characteristics, like a significant specific surface area, porous crystal structure, and relatively good thermal stability (Park et al., 2006).

ZIFs (zeolitic imidazolate frameworks) are formed from transition metal ions, and bridges are imidazolate molecules. Scientists are interested in ZIFs because they combine the best qualities of zeolite and organometallic materials, such as high porosity, large specific surface area, flexible structural change capacity (Tan, Bennett, & Cheetham, 2010), easy synthesis process, adjustable nanostructure and pore size, and high water resistance (Ighalo et al., 2022). As a result, ZIFs are considered potentially useful materials in the application of treating hazardous persistent organic substances in the aquatic environment. When oxidants are present, ZIFs act as catalysts to speed up the dissolution process, increasing the treatment's effectiveness (Li et al., 2020). Among them, Co-ZIFs is one of the most commonly studied ZIFs. Co-ZIFs have a symmetric cubic crystal structure and are constructed from the metal ion Co^{2+} and the organic compound 2-methylimidazole, where the Co^{2+} ligand acts as a secondary unit and links with organic bridges (Wang et al., 2017). With their outstanding durability and flexibility properties, Co-ZIFs have been studied for many applications, such as adsorption, sensing, drug delivery, and catalysis (Zhong et al., 2018). Co-ZIFs are frequently employed as efficient drivers to eliminating to stable organic compounds in water because of thier wide applicability. At the same time, in order to enhance the catalytic efficiency, catalytic applications are frequently implemented on modified Co-ZIFs materials. These modifications involve adding extra metal ions to the structure, doping with metal oxides, or carbonizing the framework to enhance the materials' intrinsic superior qualities and increase their catalytic potential. The enhancement of several attributes over the original ZIFs has led to the promotion of metal ion doping into the structure of Co-ZIFs in recent years. Noor's research group synthesized monometallic materials, such as Zn-ZIFs, Co-ZIFs, and bimetallic Zn/Co ZIFs (doped with Zn^{2+} and Co^{2+} ions in the same ZIFs framework), and then assessed their removal ability for six different types of dyes, including Methylene Blue, Methyl Orange, Methyl Red, Reactive Red, Rhodamine B, and Crystal Violet. This was done prove an alteration in properties that occurs when doping metal ions into monometallic ZIFs. According to the results, Zn/Co ZIFs had a greater specific surface area than Zn-ZIFs and Co-ZIFs, with corresponding values of 1738 m^2/g, 1576 m^2/g, and 1419 m^2/g. Furthermore, Zn/Co ZIFs had a higher adsorption capacity for all 6 dyes than Zn-ZIFs and Co-ZIFs (Noor, Raffi, Iqbal, Yaqoob, & Zaman, 2019). It is clear that the properties of ZIF materials were significantly better than those of monometallic materials after the metal centers were doped into the original structure. In 2018, the research team of Hu et al. successfully doped Fe into Co-ZIFs to create FeCo-ZIFs. Compared to Co-ZIFs, which had a diameter of roughly 0.4 μm, FeCo-ZIFs had a diameter of 1 μm. FeCo-ZIFs possessed a pore ability to 0.670 cm^3/g, an enormous amount of surface of 1450.8 m^2/g, and thermal stability up to 550°C (Hu et al., 2018).

FeCo-ZIFs have emerged as promising precursors for developing high-performance electrocatalysts. In 2019, Chao et al. reported the M-FeCo-N-C-0.2, based on FeCo-ZIFs, exhibited an exceptional release ability of 18,750 mAh/g and outstanding cycling stability in Li-O_2 batteries, which was attributed to the existence on macropores (Chao et al., 2019). Furthermore, Chen and colleagues (2022) demonstrated that carbonized FeCo-ZIFs could efficiently catalyze the reduction of electrons of carbon dioxide, with a carbon monoxide selectivity of 51.9%. The improved efficiency of the catalysis was put down to synergistic effect that the bimetallic centers and the carbon support's large surface area. These findings underscore the potential of FeCo-ZIFs in clean and sustainable energy technologies.

The previous study has helped to show that adding metal ions to Co-ZIFs can greatly enhance the material's qualities and increase application efficiency, particularly in terms of its viability in removing persistent materials from wastewater. The goal of this research project is to create a novel kind of catalyst using the ZIFs group material as a substrate. Specifically, the team wants to create FeCo-ZIFs by combining the Co-ZIFs substrate with Fe ion particles. The newly created substance's ability to catalytically treat CIP, when using potassium peroxydisulfate (PDS) as an oxidizing agent, will be examined.

2. MATERIALS AND METHOD

2.1. Chemicals and materials

Chemical substances used in the research was tested for purity and obtained from commercial suppliers. Ferrous sulfate heptahydrate ($FeSO_4.7H_2O$, 99%, China), methanol (MeOH, CH_3OH, 99.5%, China), cobalt (II) nitrate hexahydrate ($Co(NO_3)_2.6H_2O$, 99%, China), ciprofloxacin hydrochloride (CIP, $C_{17}H_{18}FN_3O_3.HCl.H_2O$, China), potassium peroxydisulfate (PDS, $K_2S_2O_8$, 99.5%, China), 2-

methylimidazole (2-MIm, $C_4H_6N_2$, 99%, Acros). All the experiments used deionized water.

2.2. Synthesis of FeCo-ZIFs

The solvothermal approach was used to create FeCo-ZIFs following a previously published procedure with slight modifications (Hu et al., 2018). The synthesis conditions were determined at the ambient temperature (30±2°C) with methanol solvent. Mole ratios of Fe^{2+} to Co^{2+}, and the total moles of metal salts to 2-MIm were 1:5 and 1:16, respectively. Namely, $FeSO_4.7H_2O$ (0.42 mmol) with $Co(NO_3)_2.6H_2O$ (2.08 mmol) were diluted in 30 mL MeOH to yield a uniform solution. The abovementioned mixture followed by adding dropwise to 30 mL of MeOH containing 2-MIm (40 mmol) under magnetic stirring at 350 rpm, generating reddish-violet solution. After completely mixing, the obtained suspension was kept at room temperature for a full day. The resultant solid is filtered, centrifuged, and cleaned multiple times with MeOH before drying overnight at 60°C, producing FeCo-ZIFs crystals (Figure 1). Likewise, Co-ZIFs were also prepared using the same strategy with 2.5 mmol $Co(NO_3)_2.6H_2O$ together with 40 mmol 2-MIm into 60 mL MeOH.

Besides, some other heterogeneous catalysts were synthesized basing upon previously published results, including FeZn-ZIFs (Le et al., 2023), NiZn-ZIFs (Yao et al., 2020), and CuCo-ZIFs (Dang et al., 2021).

2.3. Characterization of catalysts

The phase information of all the samples was collected by powder XRD diffraction (PXRD, Empyrean-PANanlytical powder diffractometer). FT-IR spectrum (PerkinElmerMIR/NIR Frontier instrument) of FeCo-ZIFs, Co-ZIFs, and 2-MIm were analyzed to detect the existence of functional structures on the material's surface. TGA analysis was acquired using a LabSys Evo TG-DSC 1600 instrument to examine the thermal stability of FeCo-ZIFs. SEM assessment revealed the outside morphology of the samples (Hitachi S-4800). The composition of the chemicals of FeCo-ZIFs was identified using the EDX. The Langmuir surface areas and pore structures from the material were evaluated with the nitrogen adsorption – destruction method at 77K using Quantachrome instrument. The residual concentration of CIP was measured through the UV–vis absorption spectra and the CIP removal efficiency was calculated based on the calibration curve method.

2.4. Catalytic experiments of FeCo-ZIFs

To ascertain the catalytic efficiency of FeCo-ZIFs, materials were used to activate PDS oxidant for the removal of CIP antibiotics. The catalytic test was performed by dispersing a certain dosage of FeCo-ZIFs and PDS in 10 mL of CIP at a defined initial concentration and temperature. After completing the reaction at the selected time intervals, the post-reaction solution was collected, centrifuged and filtered to separate the catalyst particulates. To optimize the CIP elimination effectiveness of the FeCo-ZIFs/PDS catalyst arrangement, The affecting factors involving dosage of catalyst (0 – 0,5 g/L), PDS amount (0,1 – 0,5 g/L), start CIP concentrations (10 – 60 mg/L), reaction duration (10 – 60 min), and heat (room temperature – 60°C) were surveyed sequentially. The concentration of CIP in the solution had been determined by a UV–Vis spectrophotometer at a wavelength of 317 nm. The elimination of the CIP was computed by the next equation:

$$\text{Removal efficiency (\%)} = (1 - C_t/C_0) \times 100 \quad (1)$$

in which C_0 (mg/L) is the starting concentration of CIP solution and C_t (mg/L) is the rest of the CIP amount at the time of reaction t. The results presented are the average performance of three experimental replicates.

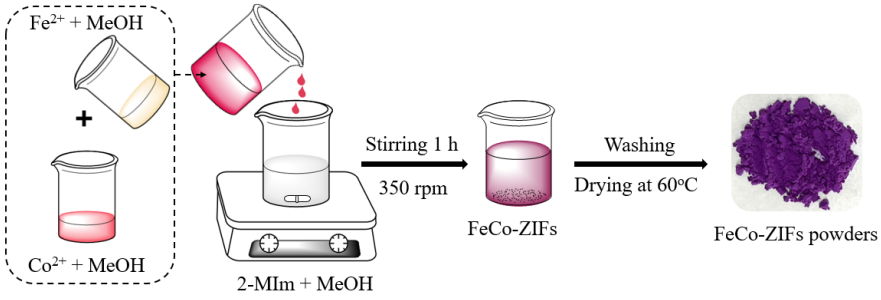

Figure 1. Depicting the fabrication of bimetallic FeCo-ZIFs

3. RESULTS AND DISCUSSION

3.1. Characterization of FeCo-ZIFs

The phase purity and crystallinity of FeCo-ZIFs were analyzed by PXRD method, and compared with single-metal Co-ZIFs (Figure 2a). As illustrated at Figure 2a, PXRD patterns of FeCo-ZIFs exhibited all the characteristic signals similar to those of Co-ZIFs. Specifically, both samples exhibited characteristic diffraction peaks at 2 theta values of 7.3°, 10.4°, 12.7°, 14.8°, 16.5°, 18.0°, 22.1°, 24.5°, and 26.7°, corresponding to the (011), (002), (112), (022), (013), (222), (114), (233), and (134) crystal facets as same as previously reported, confirming successful material synthesis and the presence of Fe^{2+} still maintained the zeolite structure of Co-ZIFs (Shams et al., 2024). Besides, sharp peaks with strong intensity were observed in patterns of PXRD of Co-ZIFs and FeCo-ZIFs without any additional phases, indicating that obtained crystals possessed high purity and crystallinity.

The FT-IR spectrum was employed to identify the groups of functions on the external surface of the catalyst, especially the coordination of the organic ligand with the metals. FT-IR spectra of FeCo-ZIFs, Co-ZIFs, and 2-MIm are displayed in Figure 2b. Results showed that almost peaks of FeCo-ZIFs and Co-ZIFs are associated with functional groups of 2-MIm. Obviously, the bending and stretching vibrations of the imidazole group characterized by the FT-IR spectra of both FeCo-ZIFs and Co-ZIFs showed peaks between 600 – 1500 cm^{-1} (Nguyen et al., 2022).

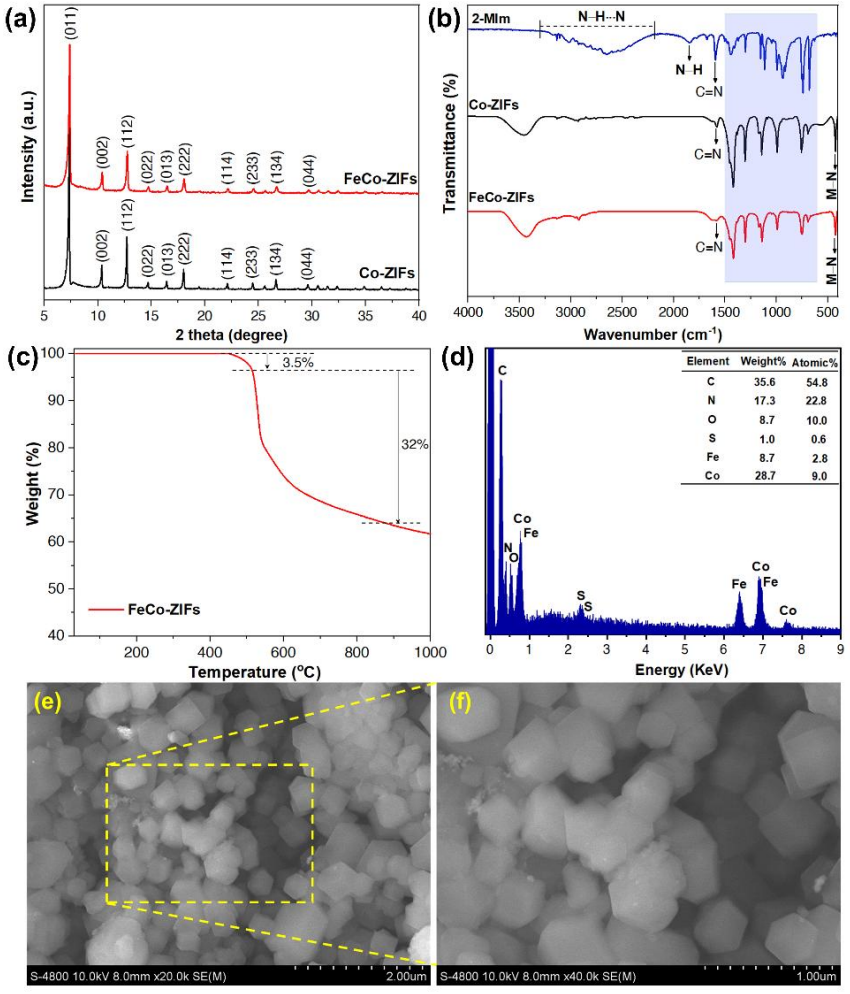

Figure 2. PXRD analysis result of Co-ZIFs, and FeCo-ZIFs (a), FT-IR spectrum of Co-ZIFs, FeCo-ZIFs, and 2-MIm (b), TGA curves from FeCo-ZIFs (c), EDX elemental analysis on FeCo-ZIFs (d), SEM pictures of FeCo-ZIFs at zoom ratios of x20,000 (e), and x40,000 (f)

The N-H stretching vibration at 1846 cm^{-1} as well as N-H···N hydrogen bond at wavenumber range of 2200 – 3300 cm^{-1} were presented in the FT-IR analysis of 2-MIm ligand, but completely disappeared in the FT-IR spectrum of FeCo-ZIFs as well Co-ZIFs, revealing that deprotonation of organic ligand to combine with metal ions (Lou et al., 2018). Supporting this assertion was the presence of the bond at the 423.7 cm^{-1} in FT-IR of Co-ZIFs and FeCo-ZIFs, which was ascribed to the bonding of the metal ion and N of 2-MIm. The FT-IR confirmed that the successful coordination of nitrogen on the 2-MIm organic bridge with Co^{2+} and Fe^{2+} metal ion nodes to form the ZIFs structure.

The thermal resistance of FeCo-ZIFs has been analyzed using TGA measures from room temperature to 1000°C and shown in Figure 2c. The results showed that FeCo-ZIFs possessed relatively high stability, with the sample weight remaining constant in the span of ambient temperature to 450°C. Initial first weight loss step was recorded at 450 – 515°C (3.5% wt%), which was attributed to gaseous molecules or unreacted species (Nguyen et al., 2022). Another significance weight loss step of 32% wt% occurred in the range from 515°C to above 800°C, which was the decomposition of the bimetallic ZIFs. Generally, FeCo-ZIFs show good thermal stability, which can be durable up to above 550°C. This makes FeCo-ZIFs a potential candidate in catalytic applications for pollutant removal. Moreover, EDX was employed to identify the elemental composition in FeCo-ZIFs. Figure 2d shows the presence about C, N, Fe, and Co elements were found in the EDS spectrum of FeCo-ZIFs, revealing that Fe^{2+} was successfully combined in the Co-ZIFs.

The morphology of FeCo-ZIFs samples were illustrated via SEM images (Figures 2e, 2f). FeCo-ZIFs showed cubic structure with regular morphology, high crystallinity, which was consisted with previous work (Hu et al., 2018). Furthermore, the obtained catalyst possessed smooth surfaces, sharp edges, and well-defined corners, demonstrating that the participation of iron ions into the Co-ZIFs framework created a homogeneous bimetallic framework. The pore volume and Langmuir surface area of FeCo-ZIFs were 1610.7 m^2/g, and 0.644 cm^3/g, respectively, which facilitated the removal efficiency of CIP.

3.2. CIP removal efficiency of FeCo-ZIFs/PDS

FeCo-ZIFs was investigated for their catalytic capacity via PDS activation process to remove CIP antibiotic. In this process, FeCo-ZIFs act as catalysts, supplying metal ions including Fe^{2+} and Co^{2+} to activate PDS, thereby generating strong oxidative radicals (i.e. $SO_4^{\bullet-}$) to target CIP molecules. Accordingly, the role of FeCo-ZIFs catalyst was considered by conducting FeCo-ZIFs dosage surveys in the range of 0 – 0.5 g/L. Experimental conditions were conducted at the fixed factors, including 0.2 g/L of PDS dose, 30 mg/L of beginning CIP concentrations at room temp (30±2°C) within 30 min (Figure 3).

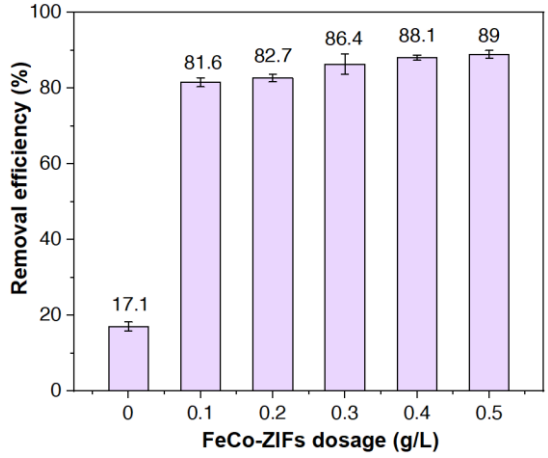

Figure 3. The CIP removal efficiency of FeCo-ZIFs/PDS in different catalyst dosages. Experimental conditions: 0.2 g/L of PDS dose, 30 mg/L of beginning CIP concentration, reaction duration of 30 min, at room temp (30±2°C)

As shown in Figure 3, the importance of FeCo-ZIFs was clearly demonstrated when CIP removal efficiency increased with the escalation of catalyst dosage. Introducing a significant amount of FeCo-ZIFs increases the number of sites that are active for PDS activation and generates more $SO_4^{\bullet-}$ for attacking CIP (Eqs. (2-5)) (Iqbal et al., 2024; Li et al., 2022; Li et al., 2021; Pirsaheb et al., 2020):

$$Fe^{2+} + S_2O_8^{2-} \rightarrow Fe^{3+} + SO_4^{\bullet-} + SO_4^{2-} \quad (2)$$

$$Co^{2+} + S_2O_8^{2-} \rightarrow Co^{3+} + SO_4^{\bullet-} + SO_4^{2-} \quad (3)$$

$$SO_4^{\bullet-} + \text{organic compounds} \rightarrow H_2O + CO_2 + SO_4^{2-} + \text{byproducts} \quad (4)$$

$$SO_4^{\bullet-} + CIP \rightarrow \text{Intermediate} \quad (5)$$

Without the use of a catalyst, the amount of CIP that was removed only reached about 17.1%, whereas this performance increased from 81.6% to 88% with the increase of FeCo-ZIFs dosage vary between 0.1

– 0.4 g/L, respectively. However, increasing the FeCo-ZIFs dosage to 0.5 g/L did not result in a substantial increase in removal efficiency. As a result 0.4 g/L of FeCo-ZIFs proved to be the optimum catalyst dosage to efficient CIP removal in this study.

Additionally, the effect of different PDS dosages (0.1 – 0.5 g/L) on removing capacity of CIP was investigated under reaction conditions including FeCo-ZIFs dose of 0.4 g/L, beginning CIP concentrations of 30 mg/L within 30 min at room temperature (30±2°C). Results are shown in Figure 4.

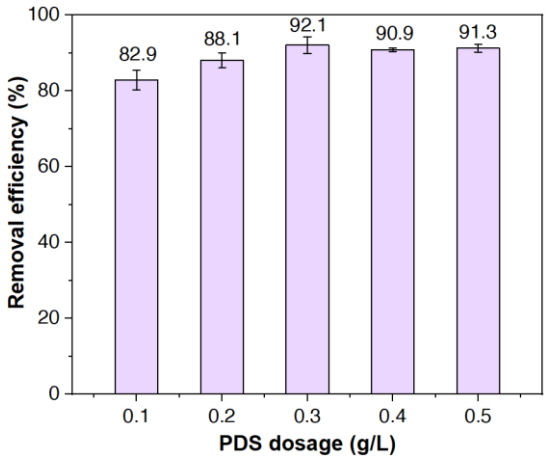

Figure 4. The CIP removal efficiency of FeCo-ZIFs/PDS in different PDS dosages. Experimental conditions: 0.4 g/L of FeCo-ZIFs dose, 30 mg/L of beginning CIP concentration, reaction duration of 30 min, at room temp (30±2°C)

As illustrated in Figure 4, increasing the PDS dose from 0.1 to 0.3 g/L increased CIP removal rates from 82.9 to 92.1%. This suggested that increasing the PDS dose increased, the sulfate radicals supply increased, leading to boost more strong oxidation agents are formed under the activation of the catalyst and improve the CIP removal efficiency. Yet when the PDS dose had been raised to 0.4 and 0.5 g/L, elimination performance dropped to around 91% due to the PDS scavenging reaction (Eq. (6,7)) (Gaoet al., 2020). Regarding cost-effectiveness and efficiency, the optimal dosage of PDS for further was 0.3 g/L of PDS dosage.

$$SO_4^{\bullet-} + SO_4^{\bullet-} \rightarrow S_2O_8^{2-} \quad (6)$$

$$S_2O_8^{2-} + SO_4^{\bullet-} \rightarrow S_2O_8^{\bullet-} + SO_4^{2-} \quad (7)$$

Following CIP removal experiments, the effect of initial CIP quantity between 10 to 60 mg/L was investigated to evaluate CIP elimination performance in the presence with 0.4 g/L FeCo-ZIFs dosage, 0.3 g/L of PDS dosage within 30 min at room temperature (30±2°C) (Figure 5).

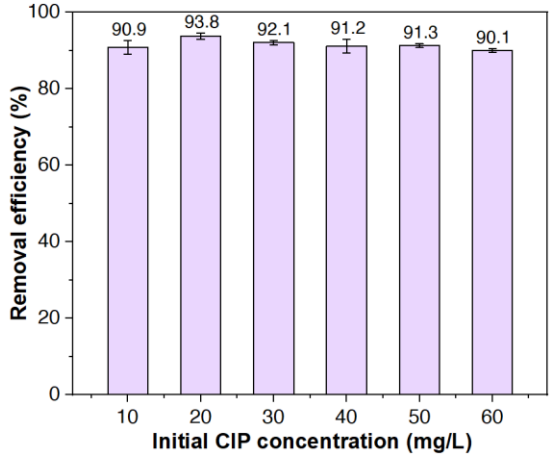

Figure 5. The CIP removal efficiency of FeCo-ZIFs/PDS in different initial CIP concentration. Experimental conditions: 0.4 g/L of FeCo-ZIFs dose, 0.3 g/L of PDS dose, reaction duration of 30 min, at room temp (30±2°C)

As depicted in Figure 5, CIP removal efficiency increased from 90.9% to 93.8% as the initial CIP concentration rose from 10 to 20 mg/L. Nevertheless, as CIP concentration increased from 30 mg/L to 60 mg/L, the CIP elimination rate declined form 92.1% to 90.1%. This could be explained that under the same optimal operating conditions at steady state, the produced amounts of oxidizing radicals by FeCo-ZIFs/PDS are constant (Sisi et al., 2020). In other words, the available $SO_4^{\bullet-}$ radical may be limited under a fixed 0.3 g/L of PDS dosage and 0.4 g/L of FeCo-ZIFs dosage, resulting in reduced CIP removal efficiency at higher CIP concentration. In this experiment, the optimal CIP concentration was chosen as 30 mg/L for further investigations.

To explore the best reaction time to remove CIP based on FeCo-ZIFs/PDS system, CIP removal experiments were conducted at different time levels (10 – 60 min) under reaction conditions including of 0.4 g/L of FeCo-ZIFs dose, 0.3 g/L of PDS dose, initial concentration CIP of 30 mg/L, at room temp (30±2°C). Results presented in Figure 6 showed that the CIP removal ability of FeCo-ZIF in the presence of PDS was achieved relatively quickly with 87.5% of CIP removed after only 10 min. When further

increased the reaction time from 10 min to 30 min, the removal performance of CIP rose from 87.5% to 92.1%. This may be due to the fact that longer reaction time facilitated the generation of more sulfate radicals to attack the CIP molecules based on the effective activation for PDS by FeCo-ZIFs. Nevertheless, excess reaction time 30 min could not only no improvement in CIP removal efficiency but also negatively affected to the overall performance of process owing to the self-quenching reaction of sulfate radicals in the solution as displayed in Eqs (6, 7). Consequently, 30 minutes was chosen as the optimum reaction time for the next studies.

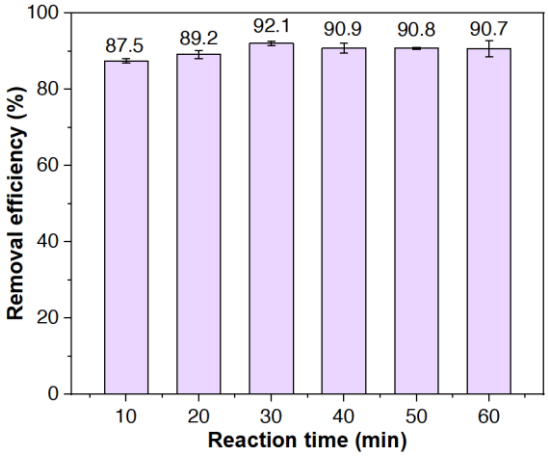

Figure 6. The CIP removal efficiency of FeCo-ZIFs/PDS in different reaction time. Experimental conditions: 0.4 g/L of FeCo-ZIFs dose, 0.3 g/L of PDS dose, initial concentration CIP of 30 mg/L, at room temp (30±2ºC)

The reaction temperature is an important parameter in advanced oxidation processes (AOPs). Hence, the effect of the reaction temp on CIP elimination was investigated with variables such as 0.4 g/L of FeCo-ZIFs dose, 0.3 g/L of PDS dose, initial concentration CIP of 30 mg/L and reaction duration of 30 minutes (Figure 7). Its CIP removal yield gained 92.1%, 90.2%, 89.2%, and 88.2% at room temperature (30±2ºC), 40ºC, 50ºC, and 60ºC, respectively. Theoretically, an increase in temperature accelerated the reaction rate, leading to faster production of sulfate radicals. However, experimental results showed that as the temperature increased, the removal efficiency decreased owing to the PDS scavenging reaction. It is noteworthy that the CIP removal performance is highest at room temperature (30±2ºC), implying that FeCo-ZIFs/PDS system can proceed easily at a relatively low energy. Considering the removal effect and cost, room temperature (30±2ºC) was determined to be the optimal temperature to remove CIP by FeCo-ZIFs/PDS.

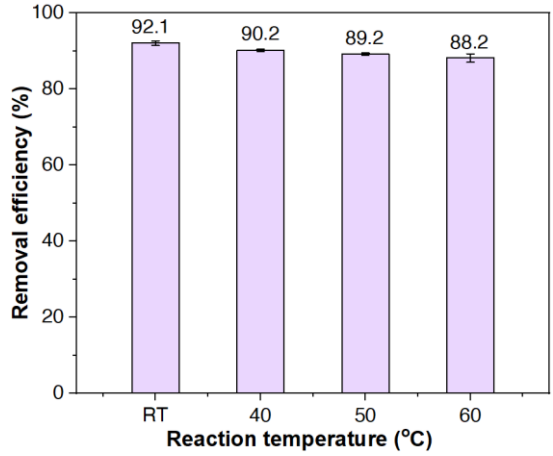

Figure 7. The CIP removal efficiency of FeCo-ZIFs/PDS in different reaction temperature. Experimental conditions: 0.4 g/L of FeCo-ZIFs dose, 0.3 g/L of PDS dose, initial concentration CIP of 30 mg/L, reaction duration of 30 min

Based on above results, FeCo-ZIFs/PDS was confirmed to be an effective catalytic system with the ability to remove 92.1% for CIP at beginning concentration at 30 mg/L during 30 min at room temp (30±2ºC) in the amount 0.3 g/L of FeCo-ZIFs and 0.4 g/L of PDS dose.

Additionally, a variety of assessments were performed using its same conditions including 0.4 g/L of catalyst, 0.3 g/L of PDS, 30 mg/L of beginning concentration CIP, for 30 minutes at room temp (30±2°C) towards evaluate that CIP elimination efficiency of different catalytic systems. In which, other catalysts used include FeZn-ZIFs, NiZn-ZIFs, CuCo-ZIFs, and Co-ZIFs. The results are presented in Table 1. The results indicated that other types of ZIF materials also possessed the potential for CIP removal in the condition of PDS. The catalytic reactions had CIP removal efficiencies of more over 80%. The achieved efficiency could be due to the structure containing of transition metal centers such as Fe^{2+}, Ni^{2+}, Cu^{2+}, Co^{2+} which were capable of activating the PDS oxidant according to the following equation (Eq. (8)) (J. Wang & Wang, 2018):

$$M^{2+} + S_2O_8^{2-} \rightarrow M^{n+1} + SO_4^{\bullet-} + SO_4^{2-} \quad (8)$$

Table 1. Comparing of CIP elimination effectiveness between FeCo-ZIFs and other catalysts

Catalyst systems	The elimination effectiveness of CIP (%)
FeCo-ZIFs/PDS	92.1±0.6
FeZn-ZIFs/PDS	79.7±1.4
NiZn-ZIFs/PDS	82.9±2.3
CuCo-ZIFs/PDS	86.1±1.6
Co-ZIFs/PDS	88.9±1.3

Overall, the FeCo-ZIFs/PDS catalyst system showed a high CIP removal efficiency, gained 92.1%, thereby confirming the significant potential of FeCo-ZIFs specifically, and zeolitic imidazole framework materials in general in the treatment of hazardous organic compounds in aqueous.

4. CONCLUSION

In conclusion, a bimetallic FeCo-ZIFs was successfully prepared and was applied just as an effective catalyst to ciprofloxacin degradation. Several approaches were used to determine the physical and chemical properties of FeCo-ZIFs. This material had a regular 12-sided rhombohedral polyhedron and was thermally stable above 550°C with Langmuir surface area was achieved 1610.7 m^2/g. Besides, the results reported that the yield decomposition of Ciprofloxacin was achieved 92.1% after 30 minutes at room temperature (30±2°C) in the condition of FeCo-ZIFs (0.4 g/L) and PDS (0.3 g/L) dosages. This therefore proves that FeCo-ZIFs are potential material in removing toxic persistent organic compounds in water, contributing to provide a sustainable method to help protect the environment.

ACKNOWLEDGMENT

The research is financed by the Can Tho University, Code: THS2024-46.

REFERENCES

Chao, F., Wang, B., Ren, J., Lu, Y., Zhang, W., Wang, X., . . . Chen, J. (2019). Micro-meso-macroporous FeCo-NC derived from hierarchical bimetallic FeCo-ZIFs as cathode catalysts for enhanced Li-O_2 batteries performance. *Journal of Energy Chemistry*, *35*, 212-219. https://doi.org/10.1016/j.jechem.2019.03.025

Chen, Z., Zhang, G., Wen, Y., Chen, N., Chen, W., Regier, T., . . . Sun, S. (2022). Atomically dispersed Fe-Co bimetallic catalysts for the promoted electroreduction of carbon dioxide. *Nano-micro letters*, *14*(1), 25. https://doi.org/10.1007/s40820-021-00746-9

Dang, H. G., Tuong, V. T., Thu, N. H. T., Van, B. N., Ho, N. T. T., & Pham, V. T. (2021). Bimetallic CuCo-Zeolitic imidazole frameworks (CuCo-ZIFs): Synthesis and characterization. *CTU Journal of Innovation and Sustainable Development*, *13*(1), 78-84. https://doi.org/10.22144/ctu.jen.2021.010

Farghal, H. H., Hassanein, D. M., Attia, A., Yacoub, N., Madkour, T., & El-Sayed, M. M. (2021). *Deploying nanoparticle-doped polymeric membranes in treating water contaminated with ciprofloxacin.* Paper presented at the Proceedings.

Gao, J., Han, D., Xu, Y., Liu, Y., & Shang, J. (2020). Persulfate activation by sulfide-modified nanoscale iron supported by biochar (S-nZVI/BC) for degradation of ciprofloxacin. *Separation and Purification Technology*, *235*, 116202. https://doi.org/10.1016/j.seppur.2019.116202

Hu, Z., Guo, Z., Zhang, Z., Dou, M., & Wang, F. (2018). Bimetal zeolitic imidazolite framework-derived iron-, cobalt-and nitrogen-codoped carbon nanopolyhedra electrocatalyst for efficient oxygen reduction. *ACS applied materials & interfaces*, *10*(15), 12651-12658. https://pubs.acs.org/doi/abs/10.1021/acsami.8b00512

Ighalo, J. O., Rangabhashiyam, S., Adeyanju, C. A., Ogunniyi, S., Adeniyi, A. G., & Igwegbe, C. A. (2022). Zeolitic imidazolate frameworks (ZIFs) for aqueous phase adsorption–a review. *Journal of Industrial and Engineering Chemistry*, *105*, 34-48. https://doi.org/10.1016/j.jiec.2021.09.029

Iqbal, J., Shah, N. S., Khan, J. A., Khan, K., Wakeel, M., Abdelghani, H. T. M., . . . Boczkaj, G. (2024). Hydroxyl and sulfate radical-based degradation of ciprofloxacin using UV-C and/or Fe^{2+}-catalyzed peroxymonosulfate: Effects of process parameters and toxicity evaluation. *Journal of Photochemistry and Photobiology A: Chemistry*, *447*, 115246. https://doi.org/10.1016/j.jphotochem.2023.115246

Le, T. T., Dang, B. H., Nguyen, T. Q., Nguyen, D. P., & Dang, G. H. (2023). Highly efficient removal of tetracycline and methyl violet 2B from aqueous solution using the bimetallic FeZn-ZIFs catalyst. *Green Processing and Synthesis*, *12*(1), 20230122. https://doi.org/10.1515/gps-2023-0122

Li, B., Wang, Y.-F., Zhang, L., & Xu, H.-Y. (2022). Enhancement strategies for efficient activation of persulfate by heterogeneous cobalt-containing catalysts: A review. *Chemosphere*, *291*, 132954. https://doi.org/10.1016/j.chemosphere.2021.132954

Li, J., Yang, L., Lai, B., Liu, C., He, Y., Yao, G., & Li, N. (2021). Recent progress on heterogeneous Fe-based materials induced persulfate activation for

organics removal. *Chemical Engineering Journal*, *414*, 128674. https://doi.org/10.1016/j.cej.2021.128674

Li, X., Yan, X., Hu, X., Feng, R., Zhou, M., & Wang, L. (2020). Hollow Cu-Co/N-doped carbon spheres derived from ZIFs as an efficient catalyst for peroxymonosulfate activation. *Chemical Engineering Journal*, *397*, 125533. https://doi.org/10.1016/j.cej.2020.125533

Lou, X., Ning, Y., Li, C., Hu, X., Shen, M., & Hu, B. (2018). Bimetallic zeolite imidazolate framework for enhanced lithium storage boosted by the redox participation of nitrogen atoms. *Sci China Mater*, *61*(8), 1040-1048. https://doi.org/10.1007/s40843-017-9200-5

Méndez-Paz, D., Omil, F., & Lema, J. (2005). Anaerobic treatment of azo dye Acid Orange 7 under fed-batch and continuous conditions. *Water research*, *39*(5), 771-778. https://doi.org/10.1016/j.watres.2004.11.022

Mondal, S. K., Saha, A. K., & Sinha, A. (2018). Removal of ciprofloxacin using modified advanced oxidation processes: kinetics, pathways and process optimization. *Journal of cleaner production*, *171*, 1203-1214. https://doi.org/10.1016/j.jclepro.2017.10.091

Nguyen, T.-B., Thai, V.-A., Chen, C.-W., Huang, C., Doong, R.-a., Chen, L., & Dong, C.-D. (2022). N-doping modified zeolitic imidazole Framework-67 (ZIF-67) for enhanced peroxymonosulfate activation to remove ciprofloxacin from aqueous solution. *Separation and Purification Technology*, *288*, 120719. https://doi.org/10.1016/j.seppur.2022.120719

Noor, T., Raffi, U., Iqbal, N., Yaqoob, L., & Zaman, N. (2019). Kinetic evaluation and comparative study of cationic and anionic dyes adsorption on Zeolitic imidazolate frameworks based metal organic frameworks. *Materials Research Express*, *6*(12), 125088. https://doi.org/10.1088/2053-1591/ab5bdf

Park, K. S., Ni, Z., Côté, A. P., Choi, J. Y., Huang, R., Uribe-Romo, F. J., . . . & Yaghi, O. M. (2006). Exceptional chemical and thermal stability of zeolitic imidazolate frameworks. *Proceedings of the National Academy of Sciences*, *103*(27), 10186-10191. https://doi.org/10.1073/pnas.0602439103

Pirsaheb, M., Hossaini, H., & Janjani, H. (2020). Reclamation of hospital secondary treatment effluent by sulfate radicals based–advanced oxidation processes (SR-AOPs) for removal of antibiotics. *Microchemical Journal*, *153*, 104430. https://doi.org/10.1016/j.microc.2019.104430

Shams, M., Niazi, Z., Saeb, M. R., Moghadam, S. M., Mohammadi, A. A., & Fattahi, M. (2024). Tailoring the topology of ZIF-67 metal-organic frameworks (MOFs) adsorbents to capture humic acids. *Ecotoxicology and Environmental Safety*, *269*, 115854. https://doi.org/10.1016/j.ecoenv.2023.115854

Sisi, A. J., Fathinia, M., Khataee, A., & Orooji, Y. (2020). Systematic activation of potassium peroxydisulfate with ZIF-8 via sono-assisted catalytic process: Mechanism and ecotoxicological analysis. *Journal of Molecular Liquids*, *308*, 113018. https://doi.org/10.1016/j.molliq.2020.113018

Tan, J. C., Bennett, T. D., & Cheetham, A. K. (2010). Chemical structure, network topology, and porosity effects on the mechanical properties of Zeolitic Imidazolate Frameworks. *Proceedings of the National Academy of Sciences*, *107*(22), 9938-9943. https://doi.org/10.1073/pnas.1003205107

Wang, J., & Wang, S. (2018). Activation of persulfate (PS) and peroxymonosulfate (PMS) and application for the degradation of emerging contaminants. *Chemical Engineering Journal*, *334*, 1502-1517. https://doi.org/10.1016/j.cej.2017.11.059

Wang, L., Guan, Y., Qiu, X., Zhu, H., Pan, S., Yu, M., & Zhang, Q. (2017). Efficient ferrite/Co/porous carbon microwave absorbing material based on ferrite@ metal–organic framework. *Chemical Engineering Journal*, *326*, 945-955. https://doi.org/10.1016/j.cej.2017.06.006

Yao, W., Guo, H., Liu, H., Li, Q., Wu, N., Li, L., . . . Yang, W. (2020). Highly electrochemical performance of Ni-ZIF-8/N S-CNTs/CS composite for simultaneous determination of dopamine, uric acid and L-tryptophan. *Microchemical Journal*, *152*, 104357. https://doi.org/10.1016/j.microc.2019.104357

Zhong, G., Liu, D., & Zhang, J. (2018). The application of ZIF-67 and its derivatives: adsorption, separation, electrochemistry and catalysts. *Journal of Materials Chemistry A*, *6*(5), 1887-1899. https://doi.org/10.1039/C7TA08268A